A Study on the Selection of Milling Cutter Material for HARDOX 500 Steel Based on Wear Using Taguchi, Entropy, and PIV Methods

Dang Thanh Tam
Faculty of Mechanical Engineering, Vinh Long University of Technology Education, Vinh Long, Vietnam
tamdt@vlute.edu.vn

Le Hong Ky
Faculty of Mechanical Engineering, Vinh Long University of Technology Education, Vinh Long, Vietnam
kylh@vlute.edu.vn (corresponding author)

Than Van The
Faculty of Mechanical Engineering, Hung Yen University of Technology and Education, Vietnam
thanthe.ck@gmail.com

Huynh Tan Dat
Can Tho Vocational College, Can Tho, Vietnam
htandat@ctvc.edu.vn

Received: 23 November 2025 | Accepted: 22 December 2025

ABSTRACT

This study investigates the selection of hard alloy insert coating materials for milling HARDOX 500 steel based on wear behavior, using a combination of Taguchi design, Entropy weighting, and the PIV multi-criteria decision-making method. Experiments were conducted on a HAAS CNC milling machine using specialized measurement equipment. The results identify the APMT1604PDER-LH insert coated with KG7016 as the most suitable option. Under the machining conditions of cutting speed v = 100 m/min and feed rate f = 0.25 mm/tooth, the KG7016-coated insert exhibited the largest flank wear (VBmax) and wear rate by mass (VM), while simultaneously achieving the lowest Surface Roughness (SR), which is symbolized with Ra. Rather than assigning equal importance to all performance criteria, the Entropy method was employed to objectively determine their relative weights, yielding values of 0.0571 for Ra, 0.4646 for VBmax, and 0.4782 for VM. These findings provide a basis for improving the service life of hard alloy cutting inserts in HARDOX 500 steel milling, particularly through the application of heating-assisted machining techniques.

Keywords-feed rate; cutting speed; coating material; wear size; wear rate

I. INTRODUCTION

Hardox 500 is a widely used wear-resistant steel manufactured by the SSAB Group (Sweden). Due to its high hardness, strength, and impact resistance, it is classified as a difficult-to-machine material with low machinability [1]. Traditionally, Hardox 500 is considered more suitable for finishing processes such as grinding or electrical discharge machining. Numerous studies have focused on grinding applications that require high dimensional accuracy and surface quality. For example, authors in [2] investigated the effects of grinding wheel dressing parameters on SR and Material Removal Rate (MRR) during the grinding of Hardox 500 steel. Increasing attention has been directed toward improving surface quality and tool performance during the milling of Hardox steels. Authors in [3, 4] studied the milling of Hardox 500 under cooling and lubrication conditions using a minimum quantity of cutting oil mixed with Al_2O_3/MoS_2 nanoparticles.

Research on cutting tool material selection and wear behavior in the machining of wear-resistant and high-hardness steels, such as Hardox 500, remains an active topic. Authors in [5] examined the influence of heat treatment conditions on the wear resistance of Hardox 500 steel. Although their work did not directly address CNC machining, the reported relationships between microstructure, hardness, and wear provide valuable insights for tribological analysis and suggest the potential of heating-assisted machining approaches.

Authors in [6] investigated the wear behavior of carbide inserts during rough milling of Hardox 500 steel, comparing different insert geometries and coatings. Authors in [7] compared Cubic Boron Nitride (CBN) and PVD-coated carbide tools when machining difficult-to-cut materials. Their findings indicate that CBN tools are generally more suitable for finishing high-hardness materials at high cutting speeds, offering extended tool life, whereas PVD-coated carbide tools are better suited for the rough machining of materials with medium hardness and for applications requiring lower tooling costs. Quantitative evaluation of tool wear is a main research topic in machining, particularly for difficult-to-machine materials. Tool wear is commonly assessed using digital imaging techniques based on wear theory [8], while gravimetric and mathematical modeling approaches are increasingly applied to estimate wear volume with higher accuracy [9, 10]. Experimental studies on Hardox 500 machining often employ response surface methods, such as the Box–Behnken design, to optimize cutting parameters [2, 3]. Multi-criteria decision-making techniques have been widely adopted to determine optimal machining conditions. For instance, authors in [11] applied the PARIS method to optimize milling parameters for SNCM439 steel based on ranked experimental results. Building on these approaches, the present study combines the Taguchi method with Entropy weighting and the PIV method to select the most suitable alloy coating material for milling HARDOX 500 steel on a CNC milling machine.

II. MATERIALS AND METHODS

A. Research Methods

a) Width of Back Wear $VBmax$

Flank wear width (VBmax) is defined as the average or maximum width of the worn region that develops on the flank face of the cutting edge. According to international ISO standards, VBmax is the most fundamental and widely used criterion for evaluating tool life. To obtain a comprehensive assessment of tool wear, VBmax measurements are often combined with gravimetric methods and detailed geometric and image analyses, such as those performed using scanning electron microscopy [8].

b) Wear Rate by Mass VM

The mass loss method is the ratio of the wear rate to the machining time:

$$VM = \frac{\Delta M}{t_m} = \frac{M_1 - M_2}{t_m} \text{ mg/min}, \quad (1)$$

ΔM (mg), ΔT (min), M_1 (mg), M_2(mg), respectively, are the amount of wear, machining time, and tool mass before and after machining. M_1 and M_2 are determined directly through the PA214 Ohaus analytical balance, and t_m is determined by [8, 13]:

$$t_m = \frac{L+L_e}{f_r}, \text{ minutes} \quad (2)$$

where L is the part length (mm), L_e is the approach length (mm), and f_r is the feed rate (mm/min).

Tool wear assessment by gravimetric measurement is an empirical technique mainly used in scientific research and academic works to quantify total material loss.

c) Taguchi Method

The Taguchi method reduces the number of experiments required while still ensuring that sufficient and reliable information is obtained using Orthogonal Arrays (OAs) [12]. By analyzing the Signal-to-Noise (S/N) ratio, the effects of input factors on the output responses can be systematically evaluated, enabling the identification of optimal process parameters. The S/N ratio is constructed and converted to calculate the following cases:

- Target value y_i to be achieved: "Bigger is better":

$$\frac{S}{N} = -10log\left(\frac{1}{n}\sum_{i=1}^{n}\frac{1}{y_i^2}\right) \quad (3)$$

- Target value y_i to be achieved: "Smaller is better":

$$\frac{S}{N} = -10log\left(\frac{1}{n}\sum_{i=1}^{n}y_i^2\right) \quad (4)$$

where n is the number of experiments.

d) Entropy Weighting Principle

According to [13], the process of calculating Entropy weight includes the following steps:

- Normalize the decision matrix (P): This is the first step to convert the original P decision matrix into a probability matrix X to ensure that the sum of the values in each column (target) is equal to 1, so that the values can be viewed as "relative probabilities" for calculating Entropy:

$$p_{ij} = \frac{x_{ij}}{\sum_{i=1}^{m}x_{ij}} \quad (5)$$

where x_{ij} is the value of the option i to the goal j and m is the number of options (experiments).

- Calculate Entropy for each target (E_i): Using Shannon's Entropy formula (measures the uniformity of data in the target j):

$$E_j = -k\sum_{i=1}^{m}(p_{ij}\, ln\, p_{ij}) \quad (6)$$

where $k = \frac{1}{ln\, m}$ (normalization constant, guaranteed $0 \le E_j \le 1$); If $p_{ij} = 0$, then by convention $ln(0)$ is handled by taking $p_{ij}\, ln\, p_{ij} = 0$.

- Calculate information dispersion (d_i): Conversion of Entropy (degree of uniformity) to dispersion (degree of usefulness).

$$d_j = 1 - E_j 7 \quad (7)$$

- E_j higher (closer to 1, uniform data), d_j lower (closer to 0, less information).
- E_j lower (closer to 0, scattered data), d_j higher (closer to 1, more information).
- Entropy weight normalization (w_j): Normalizes the values d_j to the final weight, so that the sum of the weights of all targets is equal to 1 ($\sum w_j = 1$):

$$w_j = \frac{d_j}{\sum_{j=1}^{n} d_j} \quad (8)$$

where n is the target number.

e) Theoretical Basis of the PIV Method

Suppose there are m experimental alternatives and n targets (criteria) [14]. The initial decision matrix is $X= [x_{ij}]$, where x_{ij} is the value of the alternative i with respect to the target j. According to [12], the main implementation steps are:

- Normalization of the decision matrix (R): Convert raw values into uniform values on the same scale and interest orientation (the larger the normalized value, the better).
- Standardization of the benefit objective (Maximize):

$$r_{ij} = \frac{x_{ij}}{x_j^{max}} \quad (9)$$

x_j^{max} is the largest value in the (target) column j.

- Standardization of the cost target (Minimize):

$$r_{ij} = \frac{x_j^{min}}{x_{ij}} \quad (10)$$

x_j^{min} is the smallest value in the (target) column j.

- Creation of a standardized matrix determined by (11):

$$R = [r_{ij}] \quad (11)$$

After this step, the normalized matrix $R = [r_{ij}]$ only contains values from 0 to 1, and the value 1 is always the best value for any objective.

- Constructing the weighted normalization matrix (V): The weighted impact matrix $V = [\ v_{ij}\ ]$ is calculated by multiplying the normalization matrix R with the weight vector $W = [w_1, w_2, ..., w_n]$ of the objectives:

$$v_{ij} = r_{ij} \text{x } w_j \quad (12)$$

where w_j is the weight of the target j, and $\sum_{j=1}^{n} w_j = 1$.

- Calculation of cumulative Preference Index Value (P_j): The value P_j (Preference Index Value) represents the total priority level of the option $i$across all weighted objectives.

$$P_i = \sum_{j=1}^{n} v_{ij} \quad (13)$$

The value of the option P_j, is better, because the value v_{ij} is already oriented towards benefits.

- Calculation of the Proximity Indexed Value (PIV): This step determines the final PIV, also referred to as the Composite Preference Value, by comparing the priority value (P_j) of each alternative with the ideal (maximum) and worst (minimum) values obtained from the dataset:

$$PIV_i = \frac{P_i - P^{min}}{P^{max} - P^{min}} \quad (14)$$

where:

$P^{max} = max(P_1, P_2, ..., P_m)$ (Maximum value P_i)

$P^{min} = min(P_1, P_2, ..., P_m)$ (Minimum value P_i)

where the ranking is:

- The alternative with the highest PIV_i value (closest to 1) is considered the optimal solution.
- The alternative with the highest PIV_i value (closest to 0) is regarded as the least favorable option.

B. Materials and Experimental Samples

This study used Hardox 500 steel [15], with its chemical composition, and physical and mechanical properties shown in Tables I and II.

TABLE I. CHEMICAL COMPOSITION (% MASS) [15]

C	Si	Mn	P	S	Cr	Ni	Mo	B
0.3	0.4	1.3	0.02	0.01	2.2	2	0.4	0.005

TABLE II. PHYSICAL AND MECHANICAL PROPERTIES [15]

Physical and mechanical properties	Value
Density (g/cm^3)	7.85
Yield strength (MPa)	1400
Melting point (^{0}C)	1425 – 1530
Impact toughness (J)	37
Hardness (HBW)	450 - 540
Elongation (%)	8

The experimental workpiece measuring 75 mm × 85 mm × 50 mm (Figure 1) was rough machined and chamfered 5 mm x 5 mm for even contact with the induction coil. Technical requirements: SR reaches Ra = 3.2 µm; Non-parallelism between opposing surfaces is less than 0.05 mm.

C. Cutting Tools

The experimental workpiece, with dimensions of 75 mm × 85 mm × 50 mm (Figure 1), was first rough machined and then chamfered with a 5 mm × 5 mm edge to ensure uniform contact with the induction coil. The technical requirements specified that SR should not exceed Ra = 3.2 µm and that the non-parallelism between opposite surfaces should be less than 0.05 mm.

D. Laboratory Equipment

The experimental use of the CNC milling machine HAAS VF-2 is shown in Figure 1 [16].

Fig. 1. HAAS CNC milling machine, experimental workpiece, and cutting tools.

To determine the experimental results, the study used a Mitutoyo SJ-210 SR measuring device, an Olympus GX53 metallographic microscope, and an Ohaus PA214 analytical balance to measure the SR, wear size, and alloy chip mass, as illustrated in Figure 2.

(a). (b) (c)

Fig. 2. Experimental results measuring device. (a) Olympus GX53 metallographic microscope, (b) PA214 Ohaus analytical balance, (c) Mitutoyo SJ-210 SR gauge.

E. Experimental Plan

Taguchi's L9 orthogonal matrix design method [9] was utilized with 3 input factors: cutting speed v (mm/min), feed rate f (mm/tooth), and cutting tool coating material m, as displayed in Tables I and II. The plan and results of 9 experiments are presented in Table III [17].

TABLE III. INPUT FACTOR VALUE LEVELS

Cutting parameters	**Low level**	**Middle level**	**High level**
Speed of the machine , v (m/min)	100	120	140
Knife travel , f (mm/tooth)	0.12	0.185	0.25
Cutting tool coating , m	m1	m2	m3

III. RESULTS AND ANALYSIS

A. Experimental Results

A total of 9 experiments were conducted. SR, flank wear width, and the mass of the alloy inserts were measured, and the corresponding experimental results were calculated, as depicted in Table IV.

B. Analysis of Experimental Results According to the Taguchi Method

1) With SR of the Machined Part Ra

The Analysis of the S/N ratio is displayed in Table VI and the main effect graph for the S/N ratio is shown in Figure 4. The Ra of 9 experiments shows that the cutting tool alloy material (m) does not affect the SR of the part after machining.

(a) (b)

Fig. 3. Main effects plot for S/N ratios. (a) Horizontal wear, (b) depth of wear in the horizontal direction.

TABLE IV. EXPERIMENTAL RESULTS

Run	v **(m/min)**	f **(mm/tooth)**	m	Ra **(µm)**	$VBmax$ **(mm)**	VM **(10^{-6} mg/min)**
1	100	0.12	m1	0.767	0.106	947.4
2	100	0.185	m2	0.766	0.045	500
3	100	0.25	m3	0.814	0.627	8666.7
4	120	0.12	m2	0.342	0.038	375
5	120	0.185	m3	1.562	0.206	3000
6	120	0.25	m1	1.435	0.078	1500
7	140	0.120	m3	0.473	0.072	857.1
8	140	0.185	m1	1.146	0.059	666.7
9	140	0.250	m2	1.14	0.055	857.1

TABLE V. RESPONSE TABLE FOR S/N RATIOS

Level	**v**	**f**	**m**
1	2.1369	6.0385	-0.6718
2	0.7668	-0.9161	3.4949
3	1.3908	-0.828	1.4714
Delta	1.3701	6.9546	4.1667
Rank	3	1	2

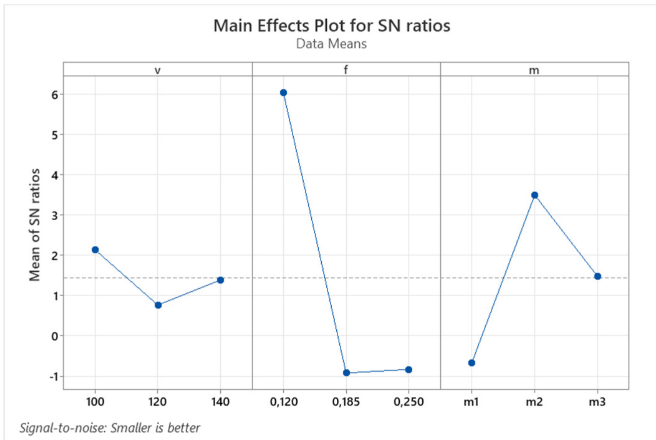

Fig. 4. Main effects plot considering the SR of the machined part.

2) With the Size of the Cutting Knife Wear $VBmax$

TABLE VI. RESPONSE TABLE FOR S/N RATIOS

Level	v	f	m
1	-16.83	-23.58	-22.08
2	-21.43	-21.75	-26.84
3	-24.21	-17.14	-13.54
Delta	7.38	6.45	13:30
Rank	2	3	1

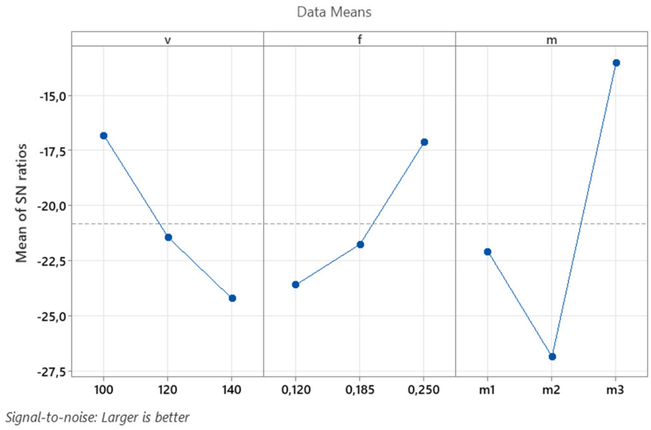

Fig. 5. Main effects plot considering the size of the cutting knife.

The analysis of the S/N ratio (Table VI) and the main effect plot for the S/N ratio (Figure 5) for the VBmax cutting tool alloy material (*m*) showed that the latter had the strongest influence on the horizontal wear size.

3) With Cutting Tool Wear Rate VM

Similarly, the analysis, presented in Table VI and Figure 6, for VM also shows that the cutting tool alloy chip material (m) has the strongest influence on the wear rate by mass. Among them, as well as for VBmax, the alloy chip coating material m3 causes the wear rate VM to increase the most intensely.

TABLE VII. RESPONSE TABLE FOR S/N RATIOS

Level	*v*	*f*	*m*
1	64.09	56.56	59.84
2	61.51	60	54.71
3	57.93	66.98	68.99
Delta	6.16	10.42	14.28
Rank	3	2	1

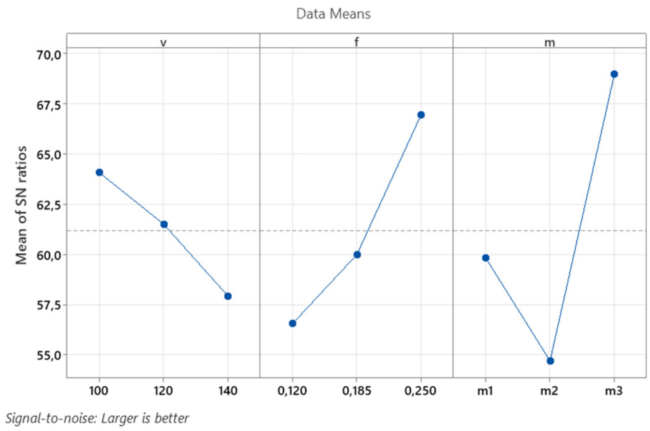

Fig. 6. Main effects plot considering cutting tool wear rate.

4) Optimize Three Goals at the Same Time

If all three objectives are assumed to have equal weight and importance, simultaneous optimization can be performed to determine a set of technological parameters, as shown in Figure 7. However, this approach yields relatively low overall and individual objective performance. In addition, without explicitly optimizing the tool coating factor (m), the results do not clearly identify the most suitable alloy coating material. Therefore, an alternative analytical approach is required to address these limitations. The combined application of the Entropy weighting method and the PIV method provides a more effective and objective solution.

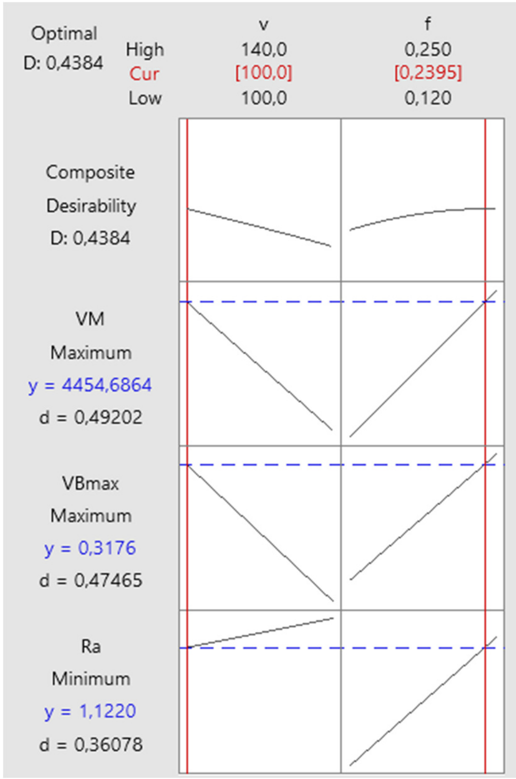

Fig. 7. Multi-objective optimization.

C. Determining the Number of the Entropy Method

There is a decision matrix, as depicted in Table VIII, from the experimental results of Table IV.

TABLE VIII. DECISION MATRIX

Run (i)	Ra	$VBmax$	VM
1	0.767	0.106	947.4
2	0.766	0.045	500
3	0.814	0.627	8666.7
4	0.342	0.038	375
5	1.562	0.206	3000
6	1.435	0.078	1500
7	0.473	0.072	857.1
8	1.146	0.059	666.7
9	1.14	0.055	857.1
$\sum x_{ij}$	8.445	1.286	17370

- Standardize the decision matrix: Apply (5) to get the results of Table IX.

TABLE IX. NORMALIZING THE DECISION MATRIX

Run (i)	p_{i1} (Ra)	p_{i2} ($VBmax$)	p_{i3} (VM)
1	0.09082	0.08243	0.05454
2	0.09069	0.035	0.02878
3	0.09639	0.48756	0.49895
4	0.0405	0.02955	0.02159
5	0.185	0.16019	0.17271
6	0.16992	0.06065	0.08636
7	0.05601	0.056	0.04934
8	0.1357	0.04588	0.03838
9	0.135	0.0428	0.04934

- Calculate Entropy (E_i) and dispersion (d_i): Use (6) and (7) with normalization constants $k = 1/ln(9) \approx 0.4551$, with the findings of Table X.

TABLE X. WEIGHTS AND DISPERSION SCORES

Target	$\sum(p_{ij}\, ln\, p_{ij})$	E_i	$d_j = 1 - E_j$
Ra	-20.64	0.9403	0.0597
$VBmax$	-11.306	0.5144	0.4856
VM	-10.991	0.5002	0.4998
$\sum d_{ij}$			1.0451

- Calculate Entropy weight: Use (8) to get the Entropy weight table for each target as Table XI.

TABLE XI. ENTROPY WEIGHTS

Target	**Weight** w_j	**Weight (%)**
Ra	0.0597/1.0451 ≈ 0.0571	5.71%
$VBmax$	0.4856/1.0451 ≈ 0.4646	46.46%
VM	0.4998/1.0451 ≈ 0.4782	47.82%
Total	1.0000	100.00%

Final Ra objective weighting results for the 3 objectives, VBmax, VM are:

$$W_{\text{Entropy}} = (0.0571, 0.4646, 0.4782)$$

The Entropy analysis shows that VBmax and VM are the dominant criteria in the evaluation process, with weights of 46.46% and 47.82%, respectively, accounting for a combined total of 94.28%. This indicates that these two wear-related indicators exhibit the greatest dispersion across the 9 experiments and, therefore, play a decisive role in distinguishing among the alternatives. In contrast, Ra contributes only 5.71% of the total weight, suggesting that its values are relatively consistent across the trials and have a much smaller influence on the overall decision compared with VBmax and VM.

D. Selection of the Milling Cutter Material with the PIV Method

From the target and weight set as Table XI, and by using (9) and (10), we get the experimental data and calculate the extreme values as Table XII. From here, we use (11) to convert all values to matrix form (in the range [0, 1]) as seen in Table XIII.

TABLE XII. DATA AND EXTREME VALUES

Run (i)	Ra **(Min)**	$VBmax$ **(Max)**	VM **(Max)**
1	0.767	0.106	947.4
2	0.766	0.045	500
3	0.814	0.627	8666.7
4	0.342	0.038	375
5	1.562	0.206	3000
6	1.435	0.078	1500
7	0.473	0.072	857.1
8	1.146	0.059	666.7
9	1.14	0.055	857.1
Extreme	$x_j^{\min} = 0.342$ $x_j^{\max} = 1.562$	$x_j^{\max} = 0.627$ $x_j^{\min} = 0.038$	$x_j^{\max} = 8666.7$ $x_j^{\min} = 375$

TABLE XIII. GOAL MATRIX

Run (i)	r_{i1} (Ra)	r_{i2} ($VBmax$)	r_{i3} (VM)
1	0.65480	0.1154	0.0682
2	0.65560	0.0119	0.0143
3	0.61590	10	10
4	10.00000	0	0
5	0.00000	0.2852	0.3113
6	0.10560	0.0848	0.1364
7	0.82730	0.0706	0.0577
8	0.34680	0.0535	0.0333
9	0.35160	0.0478	0.0577

Calculate the total weight of the weight normalization matrix according to the 3 existing objectives (0.0571, 0.4646, 0.4782) and priority score (Priority Score - P_i) according to (12), (13), to get the matrix shown in Table XIV.

TABLE XIV. NORMALIZED MATCHES AND PRIORITY POINTS

Run (i)	r_{i1}× **0.571**	r_{i2}× **0.4646**	r_{i3}× **0.4782**	P_i
1	0.03738	0.05358	0.03262	0.12358
2	0.03743	0.00552	0.00684	0.04979
3	0.03518	0.4646	0.4782	0.97798
4	0.0571	0	0	0.0571
5	0	0.13256	0.14886	0.28142
6	0.00603	0.03939	0.06524	0.11066
7	0.04724	0.03280	0.02759	0.10763
8	0.0198	0.02485	0.01593	0.06058
9	0.02008	0.02221	0.02759	0.06988

TABLE XV. OPTION RANKING

Class	**Plan**	***Pi*** **(entropy weight)**
1	Run 3	0.978
2	Run 5	0.2814
3	Run 1	0.1236
4	Run 6	0.1107
5	Run 7	0.1076
6	Run 9	0.0699
7	Run 8	0.0606
8	Run 4	0.0571
9	Run 2	0.0498

Using (14), the ranking of the alternatives is determined based on the preference index value P_j, where a larger value indicates better overall performance. The results obtained from the combined Entropy–PIV approach show that Run 3 is the optimal solution, achieving the highest P_j value of 0.9780. This outcome is reasonable because Run 3 exhibits the highest

VBmax and VM values, which together account for nearly 95% of the total weight and, therefore, dominate the decision-making process. Run 5 is identified as the second-best option with a P_j value of 0.2814. In contrast, Run 2 is ranked last, with the lowest P_j value of 0.049, due to its relatively low VBmax and VM values.

IV. CONCLUSIONS

To select an appropriate hard alloy insert coating material for milling HARDOX 500 steel, experiments were carried out on a HAAS CNC milling machine using specialized measuring equipment, following a Taguchi-based experimental design. The analysis of the experimental data using the Taguchi method indicates that the insert coating material has the most significant influence on tool wear size and wear rate. By combining the Entropy weighting method with the PIV multi-criteria decision-making technique, the study identified the APMT1604PDER-LH insert coated with KG7016 as the most suitable option. This insert exhibits the largest flank wear (VBmax) and wear rate, while simultaneously achieving the lowest Surface Roughness (SR) (*Ra*). Rather than assigning equal importance to all performance criteria, the Entropy method was used to objectively determine their relative weights, yielding values of 0.0571 for Ra, 0.4646 for VBmax, and 0.4782 for VM. These findings provide a foundation for further research aimed at extending the service life of hard alloy cutting tools in the milling of HARDOX 500 steel, with heating-assisted machining identified as a particularly promising approach.

ACKNOWLEDGMENT

The authors sincerely thank the leadership of Vinh Long University of Technology Education and the lecturers of the Faculty of Mechanical Engineering for their support and for providing favorable conditions that enabled the successful completion of this research.

REFERENCES

[1] "Your guide to Hardox® wear steel products," SSAB. https://www.ssab.com/en/brands-and-products/hardox/product-program.

[2] T. H. Danh and L. H. Ky, "Optimization of Wheel Dressing Technological Parameters when Grinding Hardox 500 Steel," *Engineering, Technology & Applied Science Research*, vol. 14, no. 4, pp. 15854–15859, Aug. 2024, https://doi.org/10.48084/etasr.7986.

[3] T. T. Long, "Experimental Investigation on Cutting Forces in Sustainable Hard Milling of Hardox 500 Steel Under Al2O3/MoS2 Hybrid Nanofluid MQCL Environment," *Lubricants*, vol. 13, no. 6, June 2025, Art. no. 240, https://doi.org/10.3390/lubricants13060240.

[4] T. M. Duc, T. N. Diep, and T. T. Long, "An experimental study on hard milling of Hardox 500 steel under Minimum Quantity Cooling Lubrication using hybrid nano cutting oil," *International Journal of Multidisciplinary Research and Growth Evaluation*, vol. 06, no. 02, pp. 347–351, Jan. 2025.

[5] M. Zemlik, B. Bialobrzeska, M. Stachowicz, and L. Konat, "Influence of heat treatment conditions of Hardox 500 steel on its resistance to abrasive wear," *Materials Science-Poland*, vol. 43, no. 1, pp. 173–195, Mar. 2025, https://doi.org/10.2478/msp-2025-0015.

[6] J. Majerik and I. Barenyi, "Experimental Investigation into Tool Wear of Cemented Carbide Cutting Inserts when Machining Wear Resistant Steel Hardox 500," *Department of Engineering, Faculty of special technology, Alexander Dubcek University of Trencin*, vol. 36, no. 2, pp. 167–174, 2016.

[7] M. Okada, A. Hosokawa, R. Tanaka, and T. Ueda, "Cutting performance of PVD-coated carbide and CBN tools in hardmilling," *International Journal of Machine Tools and Manufacture*, vol. 51, no. 2, pp. 127–132, Feb. 2011, https://doi.org/10.1016/j.ijmachtools.2010.10.007.

[8] D. A. Stephenson and J. S. Agapiou, *Metal Cutting Theory and Practice*, 3rd ed. Boca Raton: CRC Press, 2018.

[9] K. Palanikumar and J. Paulo Davim, "Mathematical model to predict tool wear on the machining of glass fibre reinforced plastic composites," *Materials & Design*, vol. 28, no. 7, pp. 2008–2014, Jan. 2007, https://doi.org/10.1016/j.matdes.2006.06.018.

[10] K. Krauze, K. Mucha, T. Wydro, J. Pawlik, and A. Wróblewska-Pawlik, "Mass and Volumetric Abrasive Wear Measurements of the Mining Conical Picks," *Sustainability*, vol. 15, no. 1, Jan. 2023, Art. no. 850, https://doi.org/10.3390/su15010850.

[11] H. K. Le, "Multi-Criteria Decision Making in the Milling Process Using the PARIS Method," *Engineering, Technology & Applied Science Research*, vol. 12, no. 5, pp. 9208–9216, Oct. 2022, https://doi.org/10.48084/etasr.5187.

[12] W. Yuin and W. Alan, "Taguchi Methods for Robust Design," *CiNii Research*, 2025, https://doi.org/10.1115/1.801578.

[13] T.-Y. Chen and C.-H. Li, "Determining objective weights with intuitionistic fuzzy entropy measures: A comparative analysis," *Information Sciences*, vol. 180, no. 21, pp. 4207–4222, Nov. 2010, https://doi.org/10.1016/j.ins.2010.07.009.

[14] S. Mufazzal and S. M. Muzakkir, "A new multi-criterion decision making (MCDM) method based on proximity indexed value for minimizing rank reversals," *Computers & Industrial Engineering*, vol. 119, pp. 427–438, May 2018, https://doi.org/10.1016/j.cie.2018.03.045.

[15] "NM400/NM450/NM500 FOB Shanghai Price: (720-930) USD/MT." https://www.baohuisteel.com/steel-products/nm400-nm450-nm500.

[16] "Fill machining center SYNCROMILL D - Economical and flexible machining of large workpieces in the smallest spaces." https://www.fill.co.at/en/products/syncromill-d.

[17] "Vosse - Manufacturer of steel structures and elements," *Vosse - Manufacturer of steel structures and elements*. https://vosse.pl/en/.